*Topic area:* **CMMSP**

# NMRON Measurements of Nano-Crystalline Cobalt

W.D. Hutchison[1], D.H. Chaplin[1], W. Dickenscheid[2] and H. Gleiter[2]

[1] *School of Physical, Environmental and Mathematical Sciences, The University of New South Wales @ ADFA, Canberra ACT 2600, Australia.*
[2] *Institut für Neue Materialien, Universität des Saarlandes, D-660 Sarbrücken, Germany.*

*e-mail of corresponding author:* w.hutchison@adfa.edu.au

## Introduction

Nanocrystalline materials are polycrystals with nanometre size crystallites and are characterised by a high density of defects and mostly incoherent interfacial regions [1]. Such material consists of two components: small crystallites and interfacial material. The atomic structure in the interfacial regions depends on the relative orientation of adjacent crystallites and since these are oriented at random there is a broad distribution of interatomic spacing within the interfaces. Therefore the interfacial component of a nano-crystalline material is a structure quite different from that formed in the glassy or bulk crystalline state of a chemically identical material.

In this paper we present the results of a microscopic study of nanocrystalline cobalt metal carried out with Nuclear Magnetic Resonance on Oriented Nuclei (NMRON) using $^{60}$Co formed *in situ* by neutron activation. In earlier work we characterised single crystal hexagonal (hcp) and polycrystalline cubic (fcc) forms of cobalt metal with NMRON [2,3]. Emphasis was placed on measuring the electric quadrupole interactions (EQI's) and therefore determining electric field gradients (efg's) at $^{60}$Co probe sites using the high resolution NMRON variant of Modulated Adiabatic Passage on Oriented Nuclei (MAPON) [4]. This emphasis is particularly appropriate for bulk cobalt since the two crystalline phases (hcp and fcc) have mean magnetic hyperfine fields differing by only a few percent, while in contrast, their respective mode EQI's differ by almost an order of magnitude due to the relatively large lattice contribution in the hcp phase. Likewise in this study of nanocrystalline cobalt, MAPON is the primary tool. However, the results of continuous wave (CW) NMRON experiments together with NMR on the stable, 100% naturally abundant, $^{59}$Co, thermally detected by nuclear orientation (NMR-TDNO), are also presented.

## Experimental Details

Nanometre particles of cobalt were produced by the inert gas evaporation technique and subsequently compacted under vacuum conditions to a bulk pellet. During this compaction process the interfacial component is built up. The pellet was ground to a powder with a particle size of a few μm. This method produced material with grain size of order 10 nm as well as preserving the interfacial component. Powder x-ray diffraction verified the small particle size and the presence of both fcc and hcp crystal phases.
Approximately 0.5 mg of the nanocrystalline cobalt powder was sealed into a silica tube under vacuum and irradiated at the HIFAR reactor, Lucas Heights, for two days at a neutron flux of 6 x $10^{13}$ cm$^{-2}$s$^{-1}$. The ambient temperature at the sample position was previously determined to be less than 80° C. Subsequently, about half of the cobalt powder (containing ~

50 μCi of $^{60}$Co) was pressed (not soldered) into the surface of a copper disc. The copper disc had been previously mechanically polished down to 0.05 μm alumina and softened by annealing at 800° C under an atmosphere of flowing hydrogen gas. The copper disc carrying the embedded cobalt was mounted with low temperature Woods metal solder to the cold finger of a dilution refrigerator together with a $^{125}$SbNi single crystal nuclear orientation thermometer. The specimen was cooled to approximately 10 mK, corresponding to ~ + 13% γ-ray anisotropy on the 428 keV line of the $^{125}$SbNi thermometer at an applied field of 0.3 T along a <111> Ni easy axis.

## Results

The maximum γ-anisotropy observed for the $^{60}$Co probes in the nanocrystalline sample was about –20% which is about one half of that expected for fully aligned cobalt at the temperature of the $^{125}$SbNi thermometer. Lack of full thermalisation of the cobalt powder is thought to be the main reason for this relatively low anisotropy. Any Kapitza boundary resistance between grains in the powder and to the copper disc, results in significant temperature differentials due to the radioactive self heating of the 50 μCi of $^{60}$Co contained within the powder.

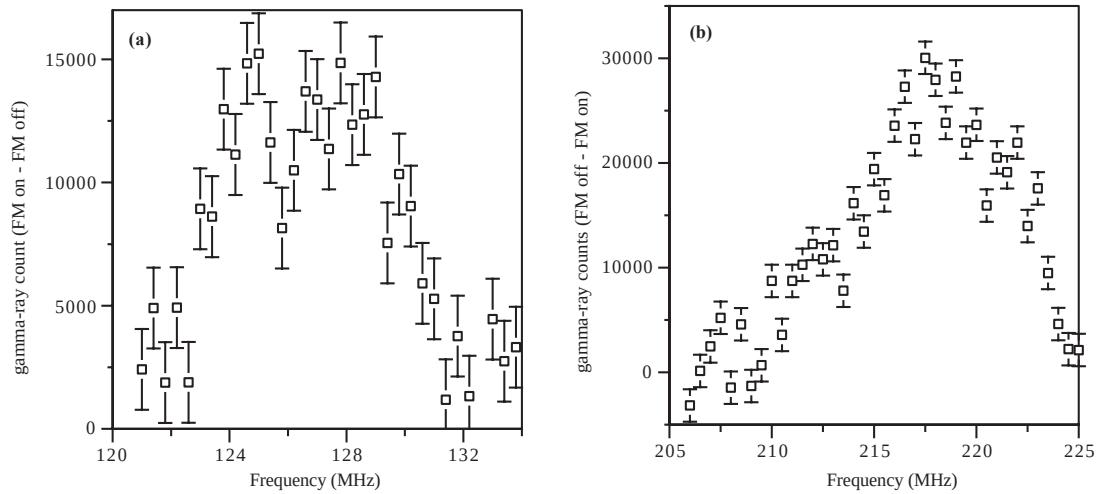


Figure 1a: CW NMRON of nanocobalt at 0.3 T applied field and FM amplitude ±200 kHz.
Figure 1b: NMR-TDNO of $^{59}$Co in the nanocrystalline powder at 0.3 T applied field.

CW NMRON for $^{60}$Co in the nanocrystalline cobalt obtained at an applied field of 0.3 T shows two peaks (Figure 1a). In general the NMR line for random hcp crystallites will be broad due to the intrinsic anisotropy in the magnetic hyperfine field. There is 0.85 T difference between crystallites with the hexagonal c axis parallel and perpendicular to the applied field direction [5]. Using the hyperfine field values for hcp cobalt of [5] and neglecting any bulk shape demagnetising field in the pressed flat powder, in a 0.3 T applied field the resonant frequencies should range from 126.08 MHz for c axis $\parallel B_{app}$ to 130.81 MHz for c axis $\perp B_{app}$. These limits fit the observed upper resonance quite well. Therefore the broad peak at the higher frequency matches that expected for polycrystalline hcp cobalt. The observed tapering off of the NMRON signal amplitude towards the higher frequency end of the resonance is due to incomplete rotation of magnetisation at the low applied field of 0.3 T. The assignment of the left hand peak is less obvious since the observed peak centre at

124.6(2) MHz differs from the expected resonant frequency of 123.23 MHz for $^{60}$Co in fcc Co at 0.3T [3,6]. Moreover, the overall Figure 1a line shape has a FWHM of ~8 MHz which is extremely broad compared with more conventional NMRON samples but is consistent with the line width of the polycrystalline, predominantly fcc, cobalt foil of [3] with the addition of a geometrically averaged hcp component.

The finely divided, thinly dispersed form of this Co powder specimen, yielding minimal rf skin effect, makes it ideal for observing NMR-TDNO (Figure 1b). This spectrum has peak destruction at 217.5(5) MHz and FWHM of 8.5(5) MHz. As for earlier NMR-TDNO of Co [7,8] the line is homogeneously broadened, the maximum signal being observed without FM. Scaling the hcp peak frequency from the CW NMRON result of Figure 1a by the $^{59}$Co/$^{60}$Co g-factor ratio it is found that the actual resonance of Figure 1b is lower by approximately 2.5 MHz. This frequency pulling is consistent with the previous NMR-TDNO studies of bulk Co. The thermometric resonance is considerably stronger for the hcp crystalline region compared with the lower frequency 'cubic' region, in contrast with the very dilute probe NMRON result.

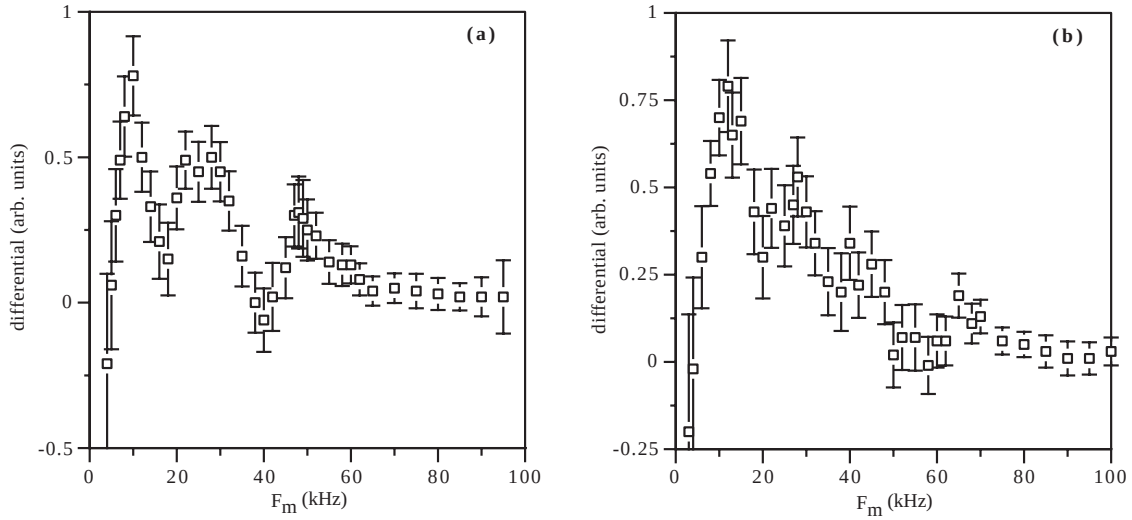


Figure 2a (2b): Analytical 13 point differentials of raw MAPON data for nanocobalt; sweeping up, 4 MHz sweep width centred on 124.5 (128.5) MHz at 0.3T applied field.

The broad nature of this magnetic frequency profile is well suited for the swept frequency techniques of adiabatic fast (single) passage and MAPON, using the $^{60}$Co probe. The most revealing results came by subdividing the sweeps into two 4 MHz sections, which largely partition in the magnetic frequency domain the majority of the hcp crystalline region from the lower frequency region. Single passage NMRON in both sweep directions was used prior to MAPON to establish optimal sweep parameters and the sign of the EQI, the latter defining the optimal MAPON sweep direction. In an applied field of 0.3 T the lower 4 MHz frequency sweep was centred at 124.5 MHz. A comparison of the post passage signals for the lower 4 MHz region indicated a discernible net negative EQI, in agreement with the known sign for $^{60}$Co in the fcc phase and in hcp with the magnetisation $\|$ to the c-axis [3]. For the higher frequency section (centred on 128.5 MHz) negligible single passage sweep asymmetry was observed suggesting an approximately even admixture of EQI signs. The MAPON spectrum differential for the lower frequency section and the higher frequency section appear in Figure. 2a and 2b respectively. In Figure 2a, three peaks are identifiable, corresponding to EQI mode values of 9.5(5), 28(2) and 48(1) kHz respectively. In Figure 2b this MAPON spectrum differential shows only one clear peak at approximately 12(2) kHz.

## Discussion

The CW NMRON result allows the nanocrystalline Co to be divided broadly into two components in the magnetic frequency domain. The upper frequency CW NMRON peak corresponds to hcp crystallites of all possible principal efg orientations with respect to the applied magnetic field. The lower frequency region includes some crystalline fcc material (as confirmed by MAPON) but is dominated by Co nuclei subject to a magnetic hyperfine field ~1% higher than that expected for fcc Co which we believe is Co nuclei sited in the interfacials. The reason for this conclusion is in part tied to the explanation for the corresponding MAPON results below. However, it is also supported by two other empirical considerations. Firstly, it may be expected that the interfacial magnetic hyperfine field would approximate more closely to the cubic value than the hcp value since both phases lack a dipolar contribution [9] to the hyperfine field. Secondly, a small difference (~2.3%) in magnetic hyperfine field between the interfacial and crystalline phases is also observed for nanocrystalline iron [10].

The lower frequency MAPON sweep (Figure 2a) covers predominantly the fcc and interfacial magnetic frequency domain. For this experiment there are three distinct EQI peaks. In general, to observe a unique peak, and hence efg, in a truly random polycrystalline material the principal efg axis must remain collinear with the direction of magnetisation; as for a (local moment generated) relativistic efg. The lowermost peak in Figure 2a matches well the relativistic EQI observed previously for polycrystalline fcc cobalt [3]. The -48 kHz EQI peak reflects minority hcp Co spins with M $\parallel$ c axis, isolated from the remaining hcp by the upper frequency limit of this lower region sweep. No such lattice based mechanism can be applied to the unanticipated peak at -28 kHz, which is not evident in the bulk phases. This relatively unique EQI is much larger than the relativistic EQI of crystalline Co (-6.2(4) kHz from fcc [2,3], -6.1(2) kHz scaled from the $^{59}$Co value of [5] for hcp cobalt) and significantly different to the hcp cobalt value with M $\perp$ c axis, where the $^{60}$Co frequency is +14.9(3) kHz [3]. This -28 kHz peak possibly reflects a relativistic EQI uniquely associated with interfacial Co sites.

## Acknowledgements

The authors acknowledge the assistance of A.V.J. Edge with specimen preparation and N. Yazidjoglou with experiments, as well as discussions with G.A. Stewart. Neutron irradiations were funded by the Australian Institute of Nuclear Science and Engineering.

[1] H. Gleiter, Nano-structured Materials **6**, 3 (1995)
[2] W.D. Hutchison, A.V.J. Edge, N. Yazidjoglou and D.H. Chaplin, Phys. Rev. Letters **67**, 3436 (1991)
[3] W.D. Hutchison, A.V.J. Edge, N. Yazidjoglou and D.H. Chaplin, Hyperfine Interact. **75**, 291 (1992)
[4] P.T. Callaghan, P.J. Back and D.H. Chaplin, Phys. Rev. B**37**, 4900 (1988)
[5] D. Fekete, H. Boasson, A. Grayevski, V. Zevin, N. Kaplan, Phys. Rev. B**17**, 347 (1978)
[6] E. Zech, E. Hagn, H. Ernst and G. Eska, Hyperfine Interact. **4**, 342 (1978)
[7] M. Willets, M. Le Gros, A. Kotlicki, G. Eska, C.E. Johnson and B.G. Turrell, Czech. J. Phys. **46**, suppl. S4, 2167 (1996)
[8] G. Seewald, E. Hagn and E. Zech, Physics Letters A**220**, 287 (1996)
[9] V. Zevin, D. Fekete and N. Kaplan, Phys. Rev. B**17**, 355 (1978)
[10] U. Herr, J. Jing, R. Birringer, U. Gonser and H. Gleiter, Appl. Phys. Lett. **50**, 472 (1987)